Supporting information

Ligand-Functionalized Organometallic Polyoxometalate

as an Efficient Catalyst Precursor for Amide Hydrogenation

Shun Hayashi*[a], Koichi Momma[b], Kiyohiro Adachi[c], Daisuke Hashizume[c]

[a]Division of Physical Sciences, Department of Science and Engineering, National Museum of Nature and Science, Ibaraki 305–0005, Japan

[b]Division of Mineral Sciences, Department of Geology and Paleontology, National Museum of Nature and Science, Ibaraki 305–0005, Japan

[c]RIKEN Center for Emergent Matter Science, Saitama 351-0198, Japan

E-mail: s-hayashi@kahaku.go.jp

List of Figures

List of Tables

Chemicals

A (pentamethylcyclopentadienyl)rhodium(III) dichloride dimer, diethyl 2,4-dimethyl-5-[(triisopropylsilyl)methylene]-1,3-cyclopentadiene-1,3-dicarboxylate, 4-acetylmorpholine, 1-acetylpiperidine, *N*-butylpropionamide, and *n*-octanamide were purchased from TCI. Rhodium(III) chloride, ammonium molybdate(VI) tetrahydrate, disodium molybdate(VI) dihydrate, and zirconium(IV) oxide were purchased from FUJIFILM Wako Chemicals. Molecular sieves (3A) were purchased from Nacalai Tesque and dried overnight at 393 K before use. γ-Al$_2$O$_3$ (JRC-ALO-8) and TiO$_2$ (JRC-TIO-17) were supplied by the Catalysis Society of Japan and calcined under static air at 773 K for 3 h before use. Deionized water (Milli-Q, >18 MΩ cm) was used in all experiments.
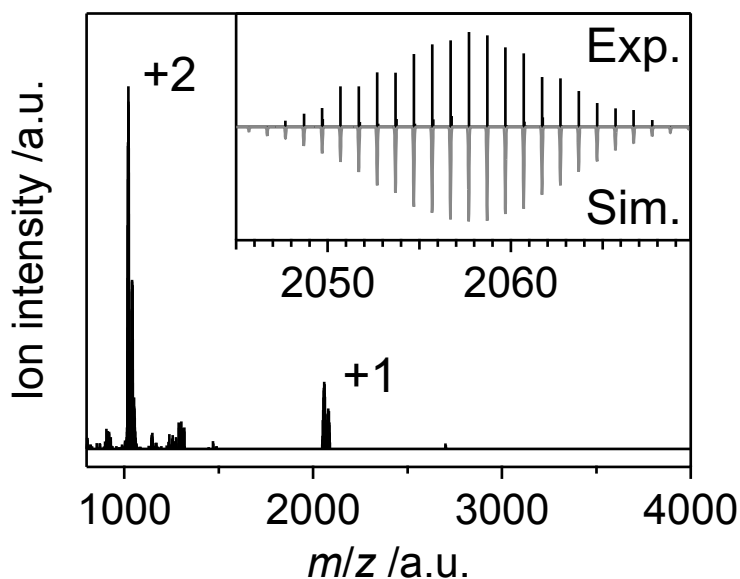
Figure S1. Positive-ion electrospray ionization mass spectrum of $[(RhCp^E)_4Mo_4O_{16}]$. Inset shows experimental and simulated isotope patterns of monovalent cation $[M+H]^+$. Divalent cations are assigned to $[M–O]^{2+}$, $[M+2H]^{2+}$, $[M+H+Na]^{2+}$, and $[M+2Na]^{2+}$.
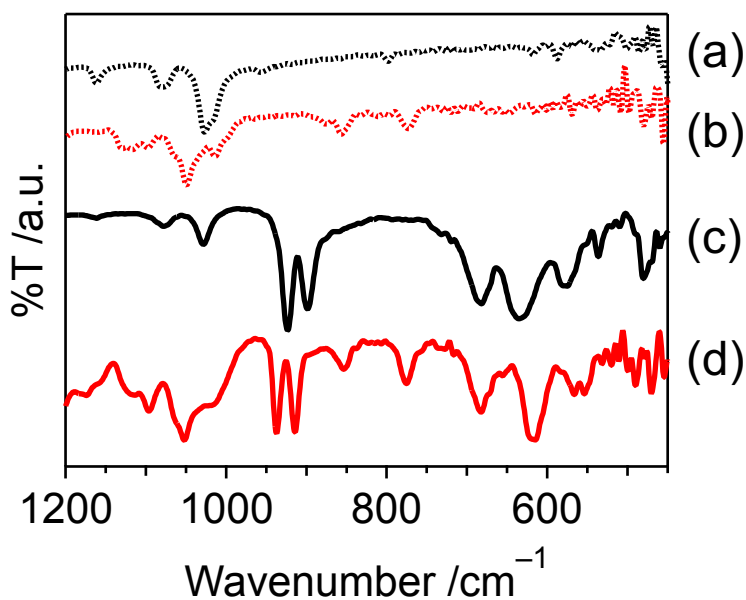
Figure S2. Fourier transform infrared spectra of (a) $[RhCp^*Cl_2]_2$, (b) $[RhCp^ECl_2]_2$, (c) $[(RhCp^*)_4Mo_4O_{16}]$, and (d) $[(RhCp^E)_4Mo_4O_{16}]$.

Figure S3. Thermal ellipsoid plot at the 50% probability level of $[(RhCp^E)_4Mo_4O_{16}]$. Hydrogen atoms are omitted for clarity.

Table S1. Data collection and details of single-crystal structural refinement

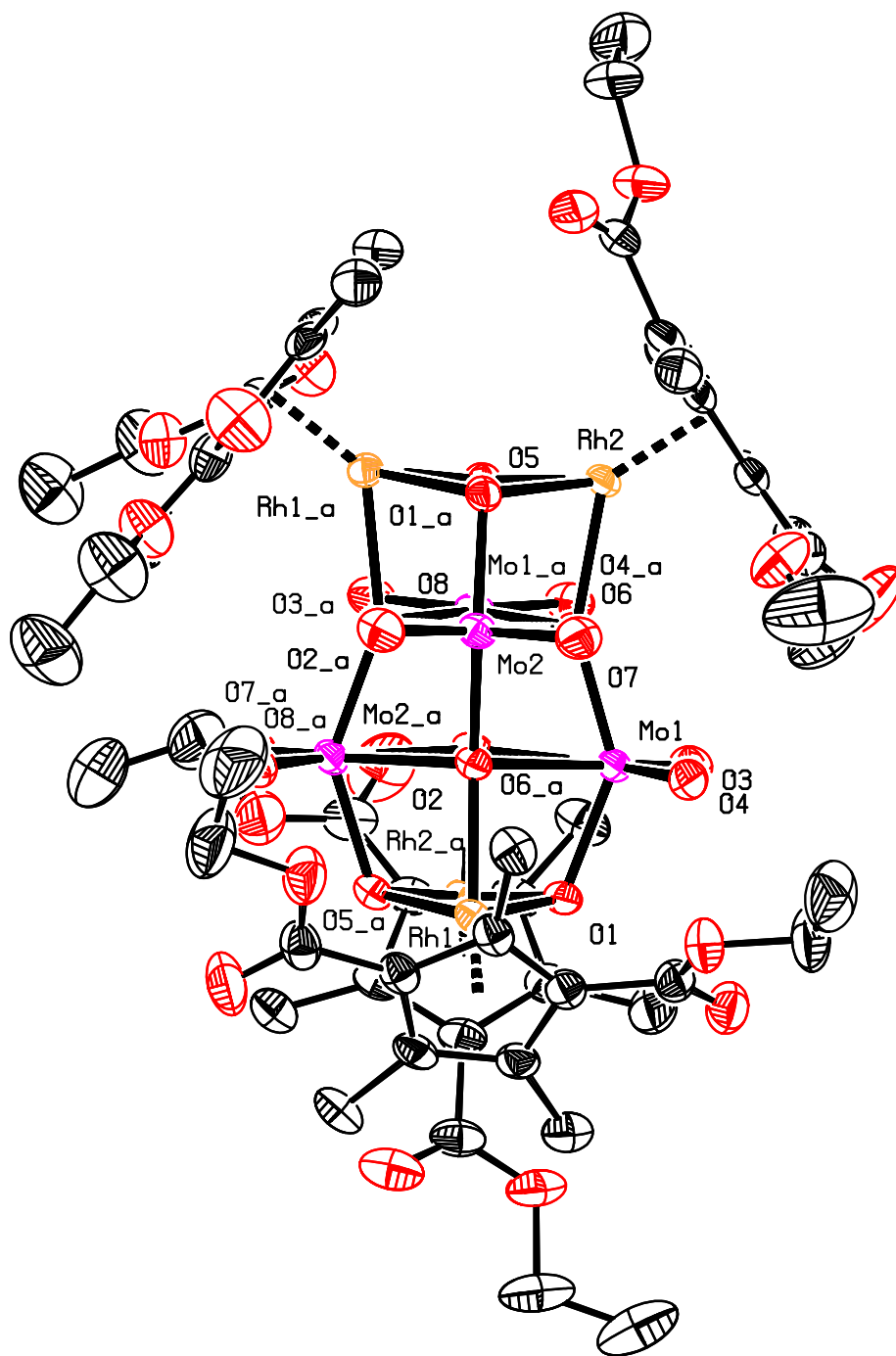| **Crystal data**	
Structural formula	$C_{28}H_{38}Mo_2O_{16}Rh_2,C_7H_8$
Space group	$C2/c$ (#15)
a /Å	24.1704(3)
b /Å	13.44359(16)
c /Å	24.7083(4)
β /°	96.3133(13)
Volume /Å^3	7979.94(18)
Z	8
D_{calc} /g/cm^3	1.865
F000	4464
μ /mm^{-1}	1.497
Crystal size /mm	0.093 × 0.07 × 0.01
Data collection	
Temperature /K	200.15
Radiation	Mo Kα (λ = 0.71073 Å)
Voltage, current	50 kV, 24 mA
θ_{max} /°	31.043
No. of reflections measured	116395
Independent reflections ($I > 2\sigma(I)$)	11226
Index ranges of h, k, and l	$-33 \leq h \leq 32, -19 \leq k \leq 18, -34 \leq l \leq 34$
Absorption correction	Numerical
Maximum and minimum transmission factors	0.863, 1.000
Refinement	
Number of variables/restraints	548 / 528
Reflection/parameter ratio	20.5
R_1, wR_2 ($I > 2\sigma(I)$)	0.0289, 0.0600
R_1, wR_2 (All reflections)	0.0474, 0.0652
Goodness-of-fit:	1.009
$\Delta\rho_{max}$, $\Delta\rho_{min}$ (e$^-$/Å^3)	0.756, −0.695
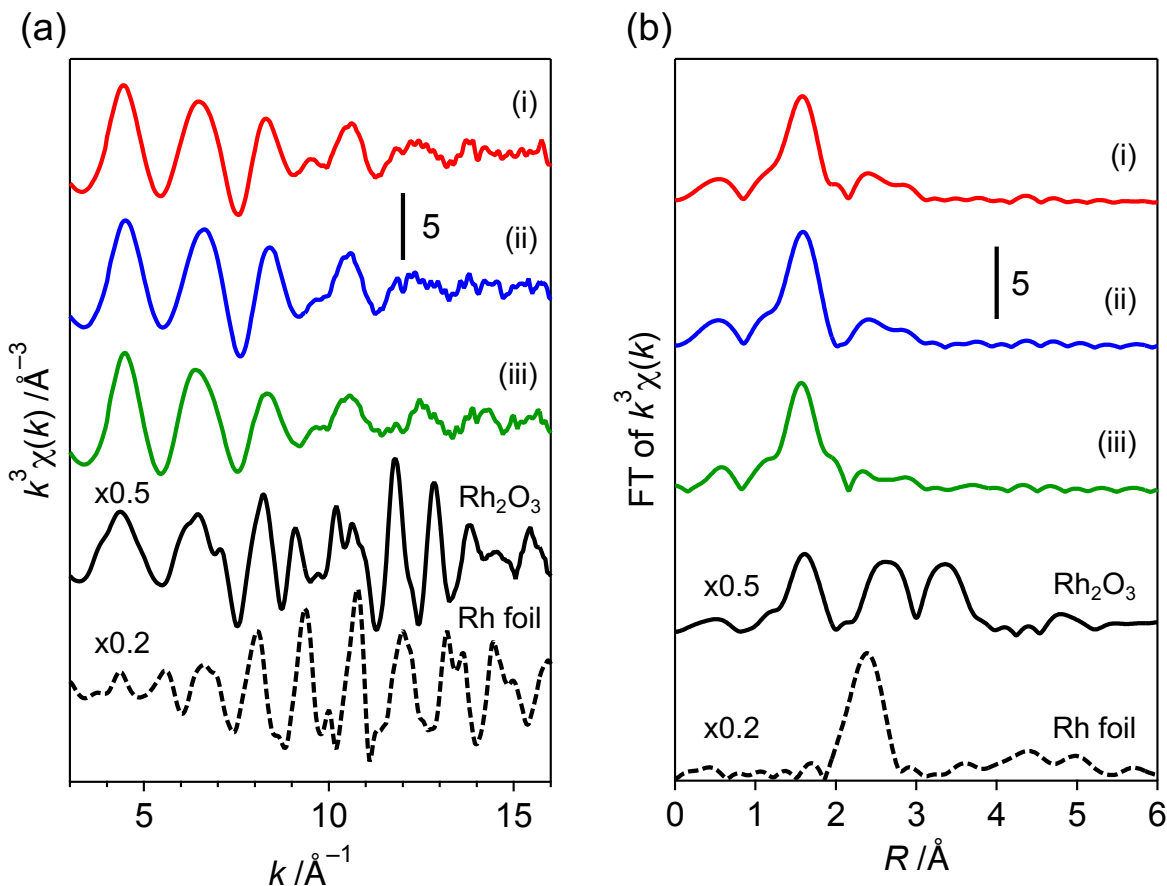
Figure S4. Rh K-edge (a) k^3-weighted and (b) Fourier transforms of extended X-ray absorption fine structure spectra of (i) $Rh_4Mo_4(Cp^E)/Al_2O_3$, (ii) $Rh_4Mo_4(Cp^*)/Al_2O_3$, and (iii) $Rh-Mo/Al_2O_3$.

Table S2. Structural parameters obtained by curve-fitting the Rh K-edge FT-EXAFS data

Compound	Bonds	CN*	r /Å[†]	σ^2 /10^{-3} Å^2[‡]	R /%[§]
$Rh_4Mo_4(Cp^E)/Al_2O_3$	Rh−O[a]	4.3(5)	2.04(1)	6(1)	3.5
$Rh_4Mo_4(Cp^*)/Al_2O_3$	Rh−O[a]	4.3(5)	2.04(1)	5(1)	3.4
$Rh-Mo/Al_2O_3$	Rh−O[a]	4.7(6)	2.04(1)	7(1)	6.2
Rh_2O_3	Rh−O[a]	5.3(5)	2.060(9)	4.0(9)	4.8
Rh foil	Rh−Rh[b]	11(2)	2.709(9)	5(1)	5.5

*Coordination number. [†]Bond length. [‡]Debye–Waller factor.
[§]$R = (\Sigma(k^3\chi^{data}(k)-k^3\chi^{fit}(k))^2)^{1/2}/(\Sigma(k^3\chi^{data}(k))^2)^{1/2}$.
r ranges for the curve-fitting analyses: [a] 1.3–1.9 and [b] 2.0–2.8 Å.

Table S3. Support effect on hydrogenation of **1a** catalyzed by Rh−Mo-based catalysts prepared from $[(RhCp^E)_4Mo_4O_{16}]$[a]

Entry	Catalyst	Yield. /%
1	$Rh_4Mo_4(Cp^E)/Al_2O_3$	45
2	$Rh_4Mo_4(Cp^E)/TiO_2$	45
3	$Rh_4Mo_4(Cp^E)/ZrO_2$	48

[a] Reaction conditions: **1a** (0.1 mmol), H_2 (0.8 MPa), 1,2-dimethoxyethane (0.5 mL), catalyst (10 mg, Rh: 0.97 mol%), molecular sieves (3A, 20 mg), 353 K, and 4 h.

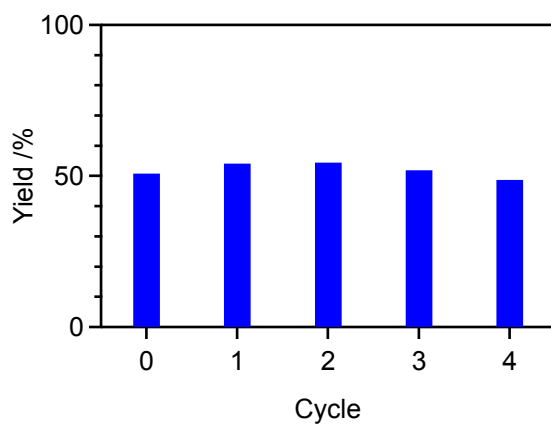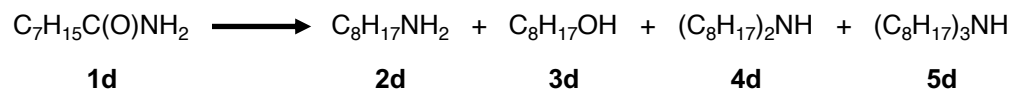Figure S5. Result of recycle tests of $Rh_4Mo_4(Cp^E)/Al_2O_3$ for hydrogenation of **1a**. Reaction conditions: **1a** (0.1 mmol), H_2 (0.8 MPa), *n*-octane (0.5 mL), catalyst (10 mg, Rh: 0.97 mol%), molecular sieves (3A, 20 mg), 353 K, and 2 h.

Table S4. Hydrogenation of *n*-octanamide catalyzed by $Rh_4Mo_4(Cp^E)/Al_2O_3$[a]

$$C_7H_{15}C(O)NH_2 \longrightarrow C_8H_{17}NH_2 + C_8H_{17}OH + (C_8H_{17})_2NH + (C_8H_{17})_3NH$$

| | **1d** | **2d** | **3d** | **4d** | **5d** |

Entry	Catalyst	Time /h	Conv. /%	Select. /%			
				2d	**3d**	**4d**	**5d**
1-1		2	26	92	5	3	-
1-2	$Rh_4Mo_4(Cp^E)/Al_2O_3$	6	72	89	4	7	-
1-3		10	97	76	3	20	1
2[b]	$Rh_4Mo_4(Cp^E)/Al_2O_3$ (Rh: 1 wt%)	6	86	69	16	15	-
3[c]	$Rh_4Mo_4(Cp^E)/Al_2O_3 + Al_2O_3$	6	75	59	7	27	8
4[d]	$Rh_4Mo_4(Cp^E)/Al_2O_3$	6	56	70	15	12	2

Reaction conditions: [a] **1d** (0.025 mmol), H_2 (0.8 MPa), *n*-octane (2 mL), catalyst (4 mg, Rh: 5 wt%, 7.8 mol%), molecular sieves (3A, 20 mg), 393 K. [b] Catalyst (20 mg, Rh: 1 wt%) was used. [c] Al_2O_3 (16 mg) was added. [d] Without molecular sieves.

Table S5. Hydrogenation of primary amines to amines

$$R-\underset{\underset{NH_2}{\|}}{\overset{O}{C}} \longrightarrow R \frown NH_2$$
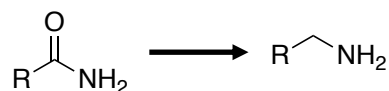
Catalyst	R	P_{H2} /MPa	Temp. /K	Time /h	Conv. /%	Select. /%	Ref.
Rh$_4$Mo$_4$(Cp^E)/Al$_2$O$_3$[a]	C7	0.8	393	10	97	76	This work
Rh$_6$(CO)$_{16}$ + Mo(CO)$_6$	Cy	10	433	16	100	87	[S1]
Ru$_3$(CO)$_{12}$ + Mo(CO)$_6$	Cy	10	433	16	100	85	[S2]
Ru$_3$(CO)$_{12}$ + Re$_2$(CO)$_{10}$	Cy	10	433	16	100	93	[S3]
Pd/Re/graphite[a]	Cy	3	433	20	21	0[d]	[S4]
Rh–MoO$_x$/SiO$_2$+CeO$_2$	Cy	8	413	4	89	62	[S5]
2Ru1W/SiO$_2$	Cy	5	433	12	94	84	[S6]
Ru-(0.2)Mo/TiO$_2$	Cy	5	433	12	83	80	[S7]
2Ru0.2Mo/SiO$_2$	Cy	5	433	12	90	75	[S8]
Rh$_6$(CO)$_{16}$ + Re$_2$(CO)$_{10}$[b]	C5	10	453	8	100	76	[S9]
RuWOx/MgAl$_2$O$_4$[c]	C2	5	473	6	96	84	[S10]
Ru/Nb$_2$O$_5$-L[c]	C2	4	453	5	100	75	[S11]
Ni$_2$Mo$_3$N[c]	C5	2	473	4	94	75	[S12]
Pt/V/HAP[a]	C7	3	343	9	50	0[e]	[S13]
Rh-V/Al$_2$O$_3$	C11	3	403	5	-	40[f]	[S14]

[a] Molecular sieves (3A or 4A) were added. [b] Diethylamine was added. [c] NH$_3$ was added. [d] A dimer formed. [e] Alcohol formed. [f] Yield. Cy = cyclohexyl, C2 = CH$_3$CH$_2$, C5 = CH$_3$(CH$_2$)$_4$, C7 = CH$_3$(CH$_2$)$_6$, and C11 = CH$_3$(CH$_2$)$_{10}$.
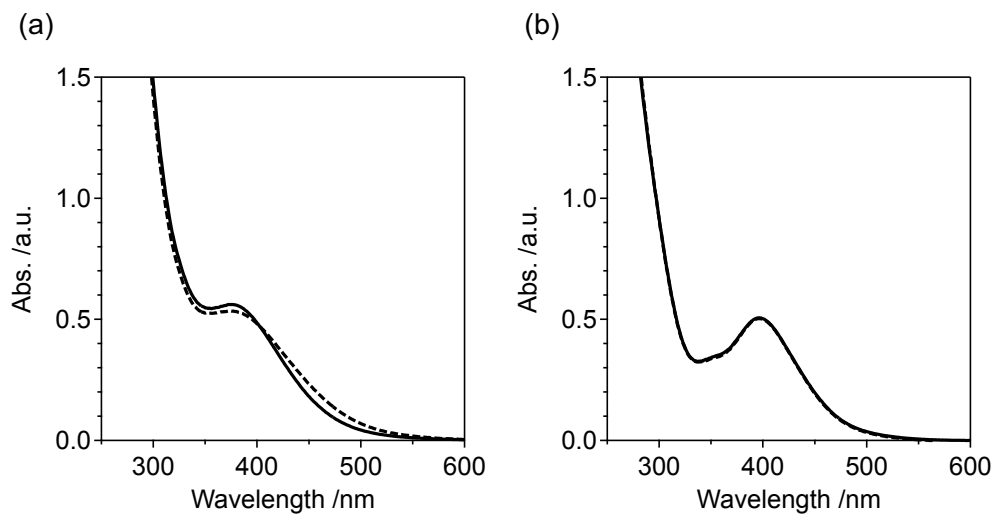
Figure S6. UV-vis spectra of the pristine precursor (dotted) and filtrate of mixture with support in MeOH (solid): (a) $[(RhCp^E)_4Mo_4O_{16}]$ and (b) $[(RhCp*)_4Mo_4O_{16}]$.
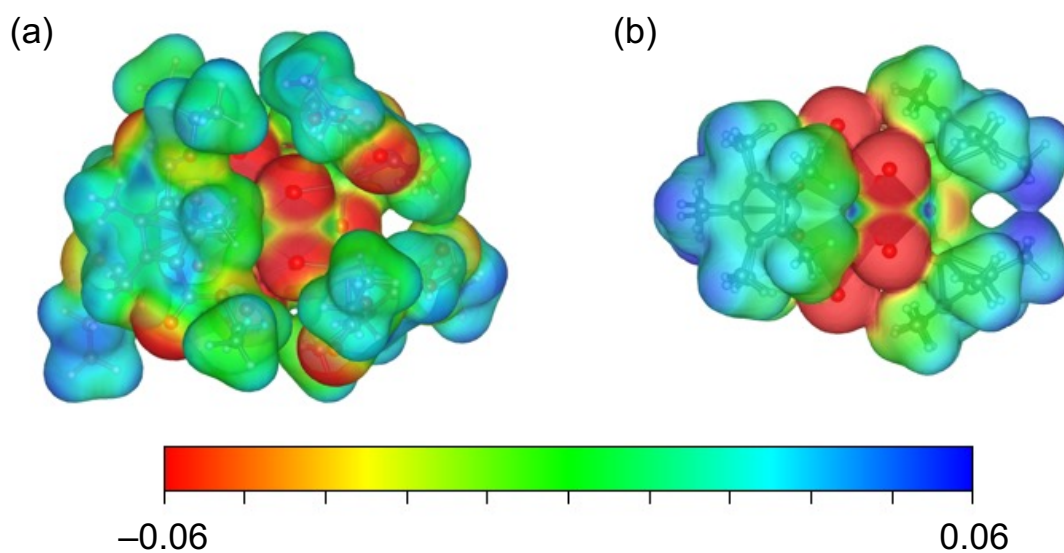
Figure S7. Electrostatic potentials mapped on electron density surfaces of (a) $[(RhCp^E)_4Mo_4O_{16}]$ and (b) $[(RhCp*)_4Mo_4O_{16}]$.

Figure S8. Representative gas chromatography chart of reaction mixture after hydrogenation of **1d** catalyzed by $Rh_4Mo_4(Cp^E)/Al_2O_3$ (Conv.: 97%, Select. to **2d:** 76%). Reaction conditions: **1d** (0.025 mmol), H_2 (0.8 MPa), *n*-octane (2 mL), catalyst (4 mg, Rh: 5 wt%, 7.8 mol%), molecular sieves (3A, 20 mg), 393 K, and 10 h.

References

(S1)   Beamson, G.; Papworth, A. J.; Philipps, C.; Smith, A. M.; Whyman, R. Selective Hydrogenation of Amides Using Rh/Mo Catalysts. *J. Catal.* **2010**, *269*, 93–102.

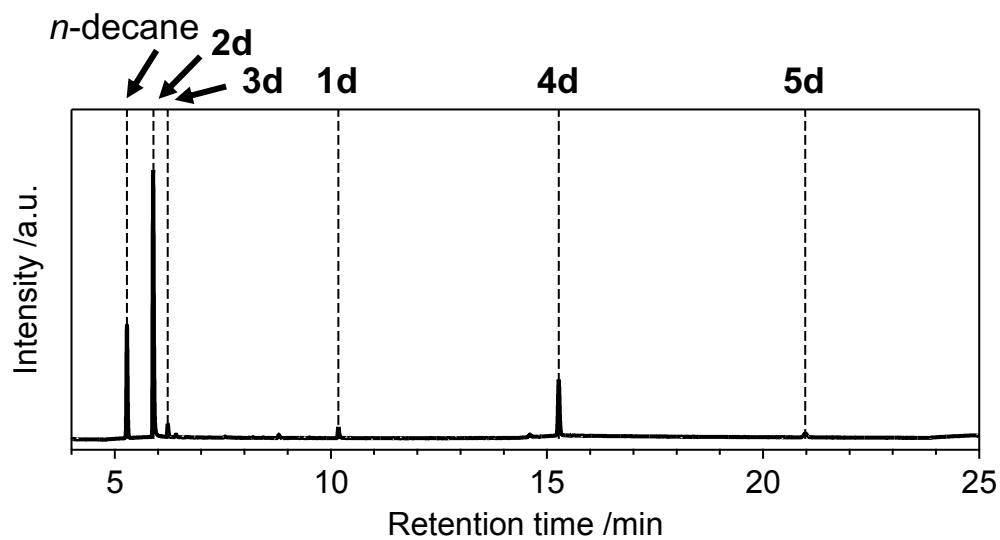(S2)   Beamson, G.; Papworth, A. J.; Philipps, C.; Smith, A. M.; Whyman, R. Selective Hydrogenation of Amides Using Ruthenium/ Molybdenum Catalysts. *Adv. Synth. Catal.* **2010**, *352*, 869–883.

(S3)   Beamson, G.; Papworth, A. J.; Philipps, C.; Smith, A. M.; Whyman, R. Selective Hydrogenation of Amides Using Bimetallic Ru/Re and Rh/Re Catalysts. *J. Catal.* **2011**, *278*, 228–238.

(S4)   Stein, M.; Breit, B. Catalytic Hydrogenation of Amides to Amines under Mild Conditions. *Angew. Chem. Int. Ed.* **2013**, *52*, 2231–2234.

(S5)   Nakagawa, Y.; Tamura, R.; Tamura, M.; Tomishige, K. Combination of Supported Bimetallic Rhodium–Molybdenum Catalyst and Cerium Oxide for Hydrogenation of Amide. *Sci. Technol. Adv. Mater.* **2015**, *16*, 014901.

(S6)   Zhang, Y.; Li, L.; Liu, F.; Qi, H.; Zhang, L.; Guan, W.; Liu, Y.; Wang, A.; Zhang, T. Synergy between Ru and WO_X Enables Efficient Hydrodeoxygenation of Primary Amides to Amines. *ACS Catal.* **2022**, *12*, 6302–6312.

(S7)   Zhang, Y.; Zhang, F.; Li, L.; Liu, F.; Wang, A. Highly Chemoselective Reduction of Amides to Amines over a Ruthenium-Molybdenum Bimetallic Catalyst. *ChemistrySelect* **2022**, *7*, e202203030.

(S8)   Zhang, Y.; Zhang, F.; Li, L.; Qi, H.; Yu, Z.; Liu, X.; Cao, C.; Liu, F.; Wang, A.; Zhang, T. Decoration of Ru Nanoparticles with Mononuclear MoO_x Boosts the Hydrodeoxygenation of Amides to Amines. *J. Catal.* **2023**, *417*, 301–313.

(S9)   Hirosawa, C.; Wakasa, N.; Fuchikami, T. Hydrogenation of Amides by the Use of Bimetallic Catalysts. *Tetrahedron Lett.* **1996**, *37*, 6749–6752.

(S10)   Coeck, R.; Berden, S.; De Vos, D. E. Sustainable Hydrogenation of Aliphatic Acyclic Primary Amides to Primary Amines with Recyclable Heterogeneous Ruthenium-Tungsten Catalysts. *Green Chem.* **2019**, *21*, 5326–5335.

(S11)   Guo, W.; Xia, Q.; Jia, H.; Guo, Y.; Liu, X.; Pan, H.; Wang, Y.; Wang, Y. Highly Selective Synthesis of Primary Amines from Amide over $Ru-Nb_2O_5$ Catalysts. *Chem. Asian J.* **2022**, *17*, e202101256.

(S12)   Yang, H.; Zhou, L.; Chen, H.; Zeng, Y.; Li, D.; Hu, C. Efficient Hydrogenation of Aliphatic Acyclic Amides to Amines by Bimetallic NiMo Nitrides via Heterogeneous Catalysis. *Chem. Eng. J.* **2023**, *473*, 145374.

(S13)   Mitsudome, T.; Miyagawa, K.; Maeno, Z.; Mizugaki, T.; Jitsukawa, K.; Yamasaki, J.; Kitagawa, Y.; Kaneda, K. Mild Hydrogenation of Amides to Amines over a Platinum-Vanadium Bimetallic Catalyst. *Angew. Chem. Int. Ed.* **2017**, *56*, 9381–9385.

(S14)   Pennetier, A.; Hernandez, W. Y.; Kusema, B. T.; Streiff, S. Efficient Hydrogenation of Aliphatic Amides to Amines over Vanadium-Modified Rhodium Supported Catalyst. *Appl. Catal. A* **2021**, *624*, 118301.